

Lipidic matrices of Essential oils: A developing strategy to preserve their biological activity and improve their stability

Sergio Cabrera¹, John Rojas^{1*}

¹College of Pharmaceutical and Food Sciences, University of Antioquia, Street 67 # 53-108, Medellín, Colombia. (J.R)

Tel.: +57-4-2195472

*Email: jrojasca@gmail.com

Abstract

Essential oils (EOs) have garnered the attention of many researchers in recent years due to their potential as complementary and alternative antioxidants, anti-inflammatory, anticancer, antibacterial, antifungal, and antiviral activities. However, their utilization is very limited due to low water solubility, evaporation, and instability to factors such as light, humidity and oxygen. This study explored the potential structuring of 20 selective EOs into lipophilic matrixes with seven different emulsifiers and determined the mechanism involved in such process. The composite Hansen parameters along with the gelling capacity, volatile retention, and oil binding ability were evaluated and analyzed by multivariate analysis. The structuring capacity mainly depended on the cohesive forces (mainly hydrogen bond interactions) of the emulsifier, which in turn was related to the radius of solubility of the EOs ($r > 0.895$). Matrixes produced with natural waxes showed the largest strength (~100%), oil binding (>97%) and volatile retention (~100%), whereas stearic acid showed the lowest values (25-30%). EOs from origanum, clove, cinnamon, and basil having large hydrogen bond forces developed the strongest lipidic matrixes. This phenomenon was attributed to the presence of an exocyclic oxygen coupled with adjacent Π electrons. EOs structuring was achieved by forming colloidal lipidic matrixes, especially with waxy emulsifiers, whereas polymeric materials only caused a partial swelling.

Keywords: Essential oils, gelling capacity, Hansen solubility, lipidic matrixes, oil binding capacity, volatile retention

INTRODUCTION

Essential oils (EOs) are natural plant products comprised of complex mixtures of biologically active substances (isoprenoids) having analgesic, sedative, anti-inflammatory, spasmolytic, antioxidant, anticancer, antibacterial, antifungal, and antiviral activities [1]. Such mixture could be represented by one major compound or different compounds in similar proportions. EOs are colorless, and volatile liquids that once applied onto the skin are easily absorbed and show great spreadability and emolliency [2]. The most effective way to use them is by external application, as gargles and mouth washes. The topical application is generally safe once formulated into a topical formulation in order to avoid irritation especially with citric oils upon exposure to the sun. They permeate membranes including the skin and have a rapid metabolism. However, their utilization is very limited due to low water solubility, evaporation, low viscosity and sensitivity to light, humidity and oxygen. Their degradation is due to cyclization, oxidation, isomerization, or dehydrogenation reactions, triggered either enzymatically or chemically, strongly influenced by processing and storage conditions of the plant material, upon distillation, or handling [3]. One efficient way to improve their stability and patient compliance is by structuring EOs with a lipidic emulsifier forming a lipidic matrix. Therefore, the formation of lipidic semi-crystalline networks traps the EOs resulting in the creation of matrix systems having different self-assembling microstructures. This study aimed to structure EOs, evaluating the structuring mechanism, oil retention, and gelling ability.

MATERIALS AND METHODS

Materials

Essential oils (i.e., orange, basil, lemon, citronella, rosemary, mint, peppermint, lavender, geranium, lavandin

grosso, thyme, clove, origanum, cardamom, lemongrass, fennel, petitgrain, clove and cinnamon) were purchase from Green Andina (Bogota, Columbia). On the other hand, emulsifiers (i.e., carnauba wax, beeswax, candelilla wax, ozokerite wax, glyceryl monostearate, stearic acid, and hydroxyethyl cellulose) were obtained from Protokimica (Medellín, Columbia).

Structuring of EOs

Approximately, 2mL of EOs was incorporated in test tubes along with 30mg (15% w/w) of the respective emulsifier. Subsequently, they were sealed and placed in the shaker (Rapidvap[®], Labconco Corp. Kansas City, MO, USA) operated at 800 rpm and 80 °C for 15 min. The tubes were then left to stand for 1 day at 25 °C in desiccators until further testing.

Gelling capacity

It was determined using an electronic caliper (sensitivity 0.01mm, Ted Pella Inc., Redding, CA) measuring the high of the remained structured matrix within the test tube once inverted 180°. If it flowed completely it was taken as 0%, whereas the absence of flow was taken as 100% gelation.

Calculation of solubility parameters

The magnitude of the dispersive (E_d), polar (E_p) and hydrogen bonding (E_h) forces for each EOs mixture and emulsifier were calculated as the weight percentage of each compound as follows:

$$\Sigma(\delta) = f^*(\delta_{di} + \delta_{pi} + \delta_{hi}) \quad (1)$$

Where, f corresponds to the fraction of the compound i within the mixture. Once values for each mixture were computed the radius of solubility (Ra) was determined as follows:

$$(Ra)^2 = 4(eo\delta_{deo} - e\delta_{de})^2 + (eo\delta_{peo} - e\delta_{pe})^2 + (eo\delta_{heo} - e\delta_{he})^2 \quad (2)$$

Where, "eo" and "e" represent the essential oil and emulsifier force type, respectively.

Morphology

The microstructure of representative lipidic matrixes was observed using an inverted phase contrast EPI microscope (IN300TC, Amscope®, Irvine, CA, USA) equipped with a 10 MP CCD low light camera at a 40X magnification.

Volatile retention capacity (VRC)

It was determined by thermogravimetry heating the previously weighed (W_{in}) samples at 40 °C for 15 min., followed by a weight measurement (W_{fin}). The VRC was quantified as follows:

$$VRC = 100\% - (100 * [W_{in} - W_{fin}] / W_{in}) \quad (3)$$

Oil binding capacity (OBC)

Approximately, 1 mL of sample was placed in a previously weighed glass tube (W_a) and was allowed to stand at 0°C for 1 h. Subsequently, the tube was weighed (W_b) and centrifuged (EBA 20, Hettich GmbH & Co, Darmstadt, Germany) at 9167 g for 15 min at room temperature. The tube was placed upside down on a filter paper for 1 h so the oil drains freely. The tube was weighted again (W_c). The OBC was calculated as follows:

$$OBC = 100\% - [(W_b - W_a) - (W_c - W_a)] / (W_b - W_a) * 100\% \quad (4)$$

Statistical analysis

The Principal Component Analysis (PCA) was used to identify and compare the relationships the theoretical physical properties and the Hansen solubility parameters of the lipidic matrixes. The software Minitab® (v. 16 Minitab, Inc, State College, PA) was used for data processing. The relationship between the different properties was assessed by the Pearson's correlation coefficient at a significance level of $p < 0.05$.

RESULTS AND DISCUSSION

Relationship between solubility parameters and EOs structuring

The dispersive, polar, and hydrogen bonding forces correspond to the Hansen solubility parameters and are denoted as a summation of cohesive forces [4,5]. Table 1 lists the magnitude of these forces for each EO. The degree of EO cohesiveness was given by the summation of these forces for each compound within the mixture.

The magnitude of the dispersive forces was larger than that of the polar and hydrogen bonding forces due to their lipophilic nature. Figure 1 depicts the gelling capacity of such EOs independent of the emulsifier type. These EOs are ranked in increasing order of hydrogen bond (δ_h) and polar (δ_p) forces. In fact, these cohesive forces affected the gelling capacity since the most resilient matrixes were located to the right of the plot. This indicates a main contribution of the hydrogen bonding forces on the structuring of geranium, origanum, basil, clove and cinnamon oils. Conversely, all other EOs showed a gelling capacity below the average since they have a low and comparable magnitude of hydrogen bond forces.

Table 1. Composition and calculated cohesive forces of essential oils

Essential oil	Compound	Composition (%)	δ_d (MPa ^{1/2})	δ_p (MPa ^{1/2})	δ_h (MPa ^{1/2})
Cardamom	1,8 Cineol	64.7	10.8	3	2.2
	Terpinyl acetate	35.27	5.9	1.5	0.9
	Total	99.97	16.7	4.5	3.1
Eucaliptus	1,8 Cineol	100	16.7	4.6	3.4
Orange	Limonene	100	17.2	1.8	4.3
Petitgrain	Limonene	100	17.2	1.8	4.3
	p-cymene	43.75	7.6	1.1	1.1
	Terpinene	27.62	4.8	0.5	1.2
	Thymol	21.38	4.1	1	2.3
Thyme	Total	92.75	16.4	2.5	4.5
	Limonene	88.55	15.2	1.6	3.8
	Pinene	5.08	0.9	0.1	0.2
	Terpineol	4.62	0.8	0.2	0.5
	Myrcene	1.75	0.3	0.03	0.04
Lemon	Total	100	17.2	2	4.5
	p-cymene	44.24	6.9	1	2.3
	1,8 Cineol	28.05	4.7	1.3	1
	Camphor	27.7	4.8	1.4	1.3
Rosemary	Total	99.99	16.4	3.7	4.6
	α -pynene	57.8	9.5	2.9	2.4
	Myrcene	42.1	6.74	0.9	2.1
Pine	Total	99.9	16.2	3.8	4.6
	Citral	72.95	11.9	1.7	4.5
	Myrcene	27.04	4.33	0.43	0.6
Lemongrass	Total	99.99	16.2	2.1	5.1
	Carvone	75	13.1	2.8	4.4
	Limonene	25	4.3	0.5	1.1

Essential oil	Compound	Composition (%)	δ_d (MPa ^{1/2})	δ_p (MPa ^{1/2})	δ_h (MPa ^{1/2})
Citronella	Total	100	17.4	3.2	5.4
	Citronelal	68.5	11.2	3.4	2.9
	Geraniol	14	2.54	0.6	1.1
	Citronelol	12.8	2.05	0.6	1.4
	Limonene	4.7	0.79	0.1	0.1
	Total	100	16.6	4.7	5.5
Mint	Menthol acetate	64.14	10.8	3	3.1
	Menthol	11.28	1.9	0.5	1.2
	Menthofuran	17.45	3	0.8	1
	Menthone	1.79	0.3	0.1	0.1
	1,8 Cineol	3.24	0.5	0.1	0.1
	Limonene	2.1	0.4	0	0.1
	Total	100	16.9	4.7	5.6
Lavender	Linalyl acetate	50	8	1.4	2.8
	Linalool	28	4.7	0.8	1.7
	Camphor	17	3	0.9	0.8
	a-terpineol	5	0.9	0.2	0.4
	Total	100	16.5	3.3	5.7
Lavandin	Linalyl acetate	50	8	1.4	2.8
	Linalool	28	4.7	0.8	1.7
	Camphor	17	3	0.9	0.8
	a-terpineol	5	0.9	0.2	0.4
	Total	100	16.5	3.3	5.7
Fennel	Anetol	86	16.8	3.8	7.7
	Limonene	9.34	1.6	0.17	0.4
	Fenchone	4.58	0.78	0.23	0.21
	Total	99.92	19.2	4.2	8.3
Geranium	Citronelol	51.5	7	2.1	4.7
	Geraniol	48.5	8.2	2	3.7
	Total	100	15.2	4.1	8.4
Oreganum	Carvacrol	92.8	17.63	4.18	10.02
	Thymol	3.5	0.67	0.16	0.38
	Cymene	2.7	0.47	0.07	0.06
	Pinene	1	0.17	0.02	0.04
	Total	100	18.9	4.4	10.5
Basil	Linalol	100	16.3	4.4	11.2
Clove	Eugenol	97.24	18.5	7.29	12.6
	B-caryophyllene	2.76	0.47	0.03	0.1
	Total	100	18.9	7.3	12.7
Cinnamon	Cinnamaldehyde	100	19	7.5	13

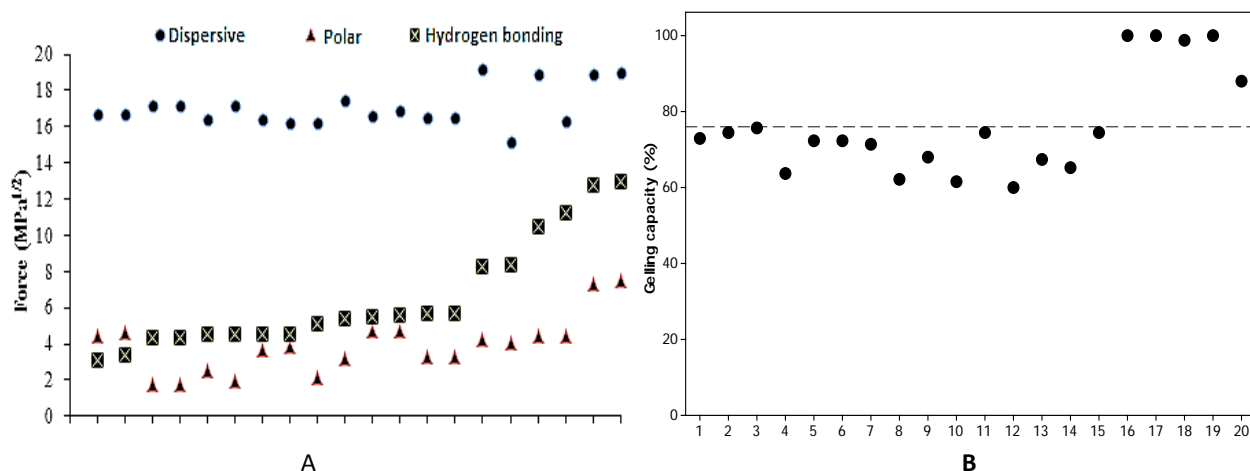


Figure 1: Cohesive forces for each essential oil mixture (A); gelling capacity (B). 1 cinnamon, 2 eucaliptus, 3 oreganum, 4 petigrain, 5 thyme, 6 lemon, 7 rosemary, 8 pine, 9 lemongrass, 10 spearmint, 11 citronella, 12 mint, 13 lavender, 14 lavandin, 15 fennel, 16 geranium, 17 origanum, 18 basil, 19 clove 20 cinnamon

Figure 2 depicts the average contribution of each emulsifier independent of the EO type. Natural waxes showed the most remarkable gelling capacities. This phenomenon is explained by their diverse chemical composition. In fact, most of them are composed of long chain esters and free fatty acids, hydrocarbons and fatty alcohols. As a result, the magnitude of the cohesive forces matched those of most EOs (Fig. 1a, oils 1-14). Conversely, low chain emulsifiers such as stearic acid and glyceryl mono-stearate showed much lower gelling capacities due to the low molecular weight and single chain length. Interestingly, hydroxyethyl cellulose (HEC), which is a hydrophobic polymer interacted mainly via hydrogen bonds with the EOs, but did not show a good gelling capacity which in turn was governed by partial swelling of the polymer [6,7].

Figure 3 shows the effect of EOs and emulsifiers on the volatile retention capacity (VRC). These matrixes exhibited a high VRC indicating a good stability for short period of times under storage. Interestingly, natural waxes showed the largest VRC (>93%) mainly attributed to their long chain fatty compounds which capture the EOs compounds within their chains. On the contrary, stearic acid presented the lowest VRC due to the short and single carbon chain which was insufficient to permanently retain the oil. Glyceril monoestearate was the only short chain ester which showed a good VRC as compared to HEC whose swelling ability favored the VRC. This phenomenon could be explained by its amphiphilic nature and thus the lipophilic chains interact with the planar cyclic oil compounds, whereas the polar zone interact with the oxygen moieties.

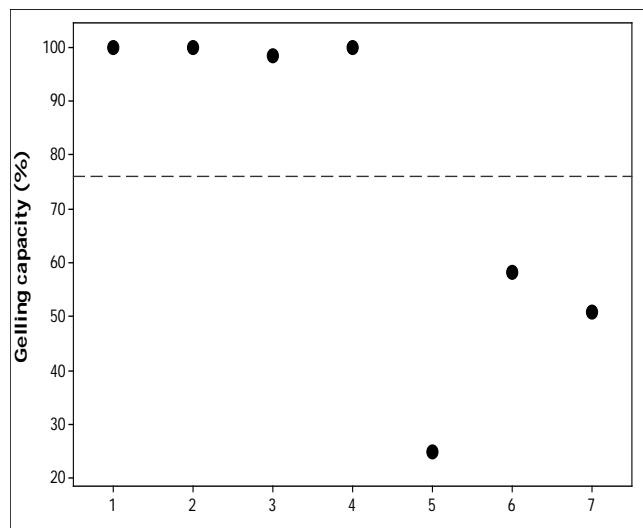


Figure 2: Gelling capacity of each emulsifier independent of the essential oil type. 1 beewax, 2 carnauba wax, 3 candelilla wax, 4 ozokerite wax, 5 stearic acid, 6 glyceryl monostearate, 7 hydroxyethyl cellulose

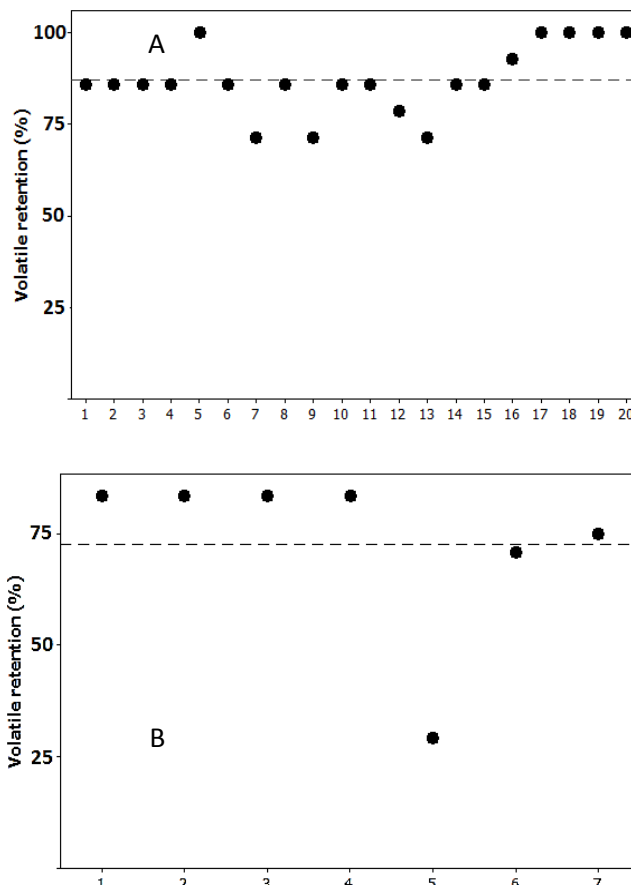


Figure 3: (A) Effect of essential oils on the volatile retention capacity. 1 cinnamon, 2 eucaliptus, 3 oreganum, 4 petigrain, 5 thyme, 6 lemon, 7 rosemary, 8 pine, 9 lemongrass, 10 spearmint, 11 citronella, 12 mint, 13 lavender, 14 lavandin, 15 fennel, 16 geranium, 17 origanum, 18 basil, 19 clove 20 cinnamon (B). Effect of emulsifiers on the volatile retention capacity. 1 beewax, 2 carnauba wax, 3 candelilla wax, 4 ozokerite wax, 5 stearic acid, 6 glyceryl monostearate, 7 hydroxyethyl cellulose

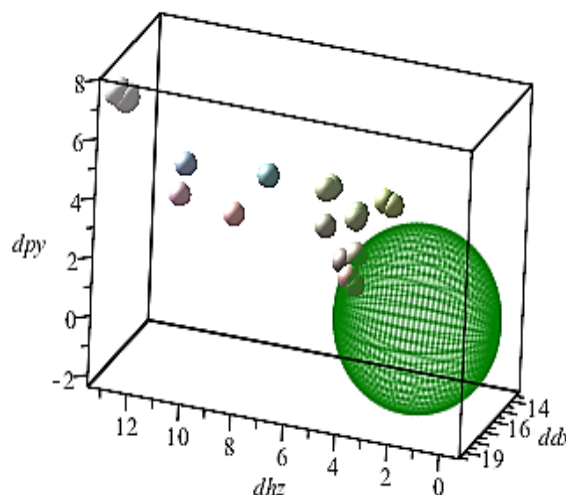


Fig 4(A)

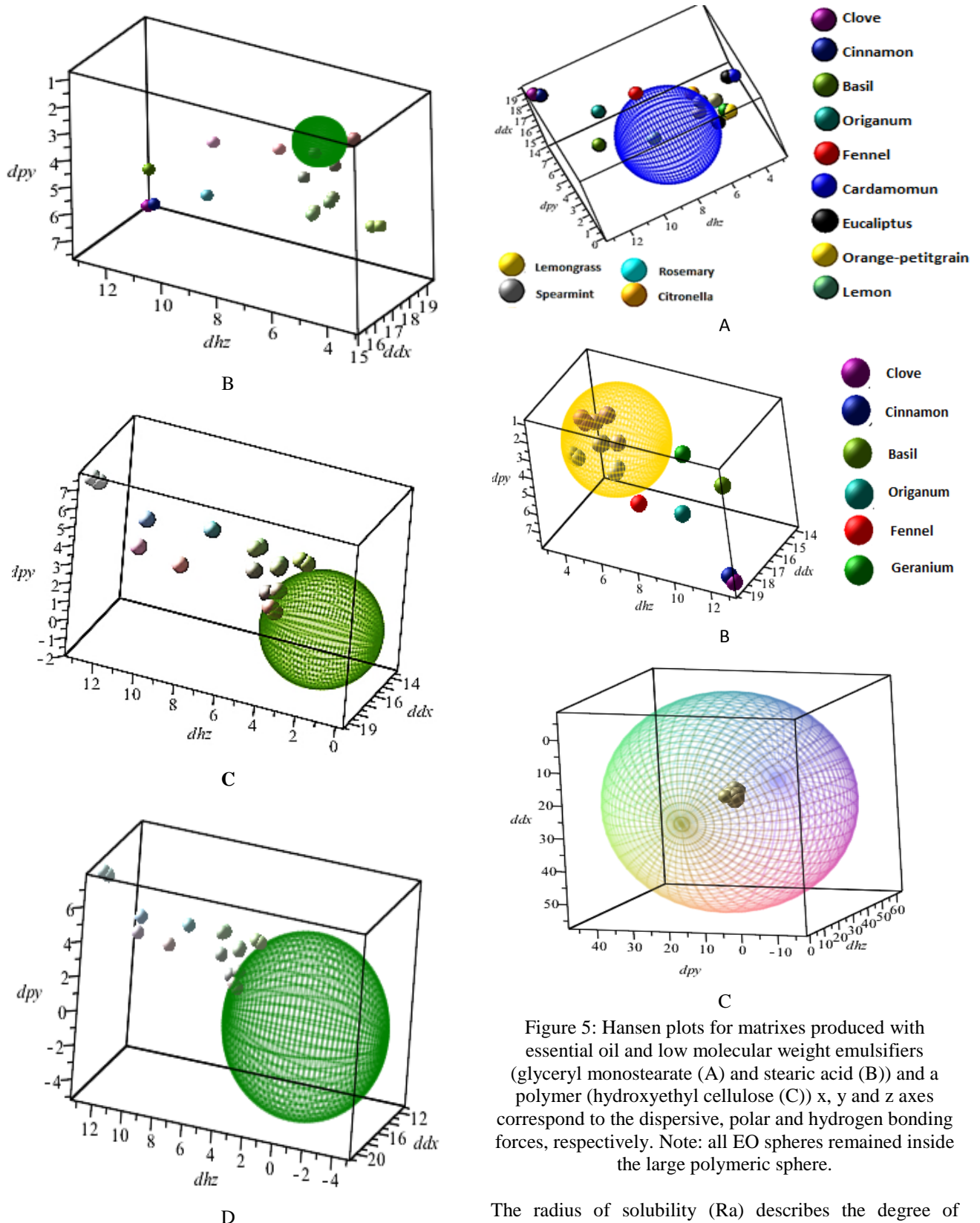


Figure 4: Hansen plots for matrixes produced with essential oil and natural waxes. (A) beeswax, (B) carnauba wax, (C) candelilla wax, (D) ozokerite wax. x, y and z axes correspond to the dispersive, polar and hydrogen bonding forces, respectively. Note: all EOs remained outside of the large wax sphere.

Figure 5: Hansen plots for matrixes produced with essential oil and low molecular weight emulsifiers (glyceryl monostearate (A) and stearic acid (B)) and a polymer (hydroxyethyl cellulose (C)) x, y and z axes correspond to the dispersive, polar and hydrogen bonding forces, respectively. Note: all EO spheres remained inside the large polymeric sphere.

The radius of solubility (R_a) describes the degree of affinity between the emulsifier and oils and has been used to predict miscibility of some compounds within organic solvents [8]. In this study it was used for the first time to compare and predict the degree of structuring between the emulsifier and the EO. Thus, it is expected a good structuring process if this R_a is large. Results indicate that fatty emulsifiers formed semi-crystalline particles upon

cooling leading to self-assembling in a 3D colloidal network structuring the EOs. Thus, a high oil structuring was anticipated when partial dissimilarity between cohesive forces (mainly hydrogen forces) between EOs and emulsifiers took place, restricting miscibility between these components followed by a large crystallization upon cooling. The net result in the Ra plot is a large distance between the emulsifier sphere and those of EOs (Fig. 4), especially when carnauba wax was employed, whereas ozokerite wax showed a reduced degree of structuring. Likewise, fatty esters such as glyceryl monostearate showed a large difference of cohesive forces with most EOs resulting in a good structuring, whereas the opposite effect occurred for stearic acid (Fig. 5a,b). On the other hand, HEC showed the largest Ra englobing all the EOs spheres as a result of the large affinity between δp and δh forces [9]. This phenomenon was reflected on a partial swelling of the microfibers resulting in rapid gelation at room temperature, especially with EOs showing high δh forces (Fig. 5c).

Figure 6 illustrates the microphotographs for the general structuring mechanism for selected emulsifiers. Polymeric materials structured EOs via rapid swelling of fibers at room temperature mediated by high δh . Conversely, fatty emulsifiers such as natural waxes required a heating and cooling cycle for the formation of crystals which in turn formed aggregates mainly by Van der Waals interactions.

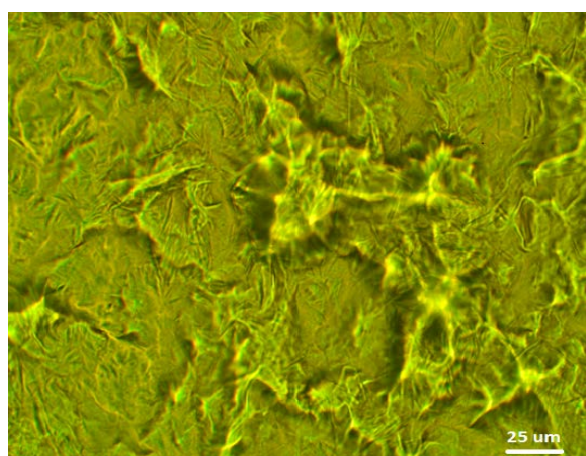
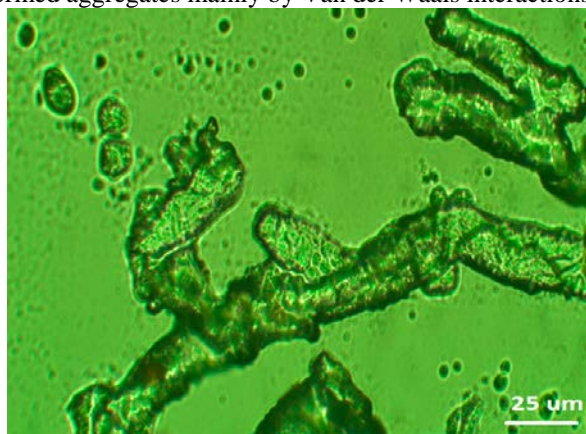
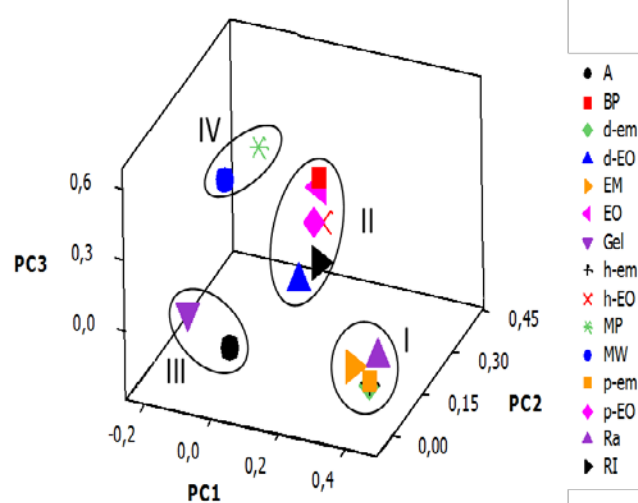


Figure 6: Microphotographs of matrixes produced by selected emulsifiers (A) Polymeric material (HEC) (B) Natural waxes

Multivariate Analysis: In order to understand the relationship between the Hanson parameters and the physical properties of the EOs and emulsifiers a principal component analysis (PCA) was undertaken. The PCA plot is illustrated in Figure 7. The first three components explained 74.4% of the data variability. All variables can be grouped into four significant clusters. The first one (I) directly correlates Ra with the cohesive forces of the emulsifier. The second cluster (II) was mainly composed by the EOs and their cohesion parameters. The third cluster (III) relates the gelling capacity with the volatile retention, whereas the last cluster (IV) associates the EOs melting point with the molecular weight of their main oil constituent. The inset table within the figure lists the most correlated variables. In this case, the cohesive parameters of the emulsifier were strongly correlated with Ra, whereas δ_h was the most influential force for the EOs.



Factor pair	r
EOs & Eh-EO	0.895
Emulsifier & δ p-emulsifier	0.823
δp -emulsifier & δd emulsifier	0.985
δh -emusifier & δd -emulsifier	0.984
δd -emulsifier & Ra	0.933
δp -emulsifier & δh -emulsifier	0.993
δp -emulsifier & Ra	0.901
δh -emulsifier & Ra	0.895
δd -emulsifier & Ra	0.933
Eh-EO & BP	0.712
Eh-EO & RI	0.736

Figure 7: Principal component Analysis Plot (CP1: 30.2%, CP2: 27.9%, CP3: 12.8%, variability). A, volatile retention; BP, boiling point; d-em, dispersive force emulsifier; d-EO, dispersive force EO; EM, emulsifier; EO, essential oil; Gel, gelling capacity; h-em, hydrogen force emulsifier; h-EO, hydrogen force EO; MP, melting point; MW, molecular weight; p-em, polar force emulsifier; p-EO, polar force EO; Ra, Solubility radius; RI, refraction index.

The first three components are explained as follows:

$$PC1 = 0.41EOs + 0.43 \delta_h -EOs + 0.403BP + 0.40 IR \quad (5)$$

$$PC2 = (0.41EM) + (0.45 \delta_d -EM) + (0.45 \delta_p -EM) + (0.45 \delta_h -EM) + (0.42 Ra) \quad (6)$$

$$PC3 = (-0.61MP) + (-0.64MW) \quad (7)$$

Where, BP, RI, EM and MW correspond to the melting point, EO refraction index, emulsifier, and EO molecular weight of the main oil component, respectively. PC1 explained the high variability mainly due to the EOs δ_h , which impacted physical properties such as IR and BP. Further, PC2, elucidates the variability of the emulsifier according to the cohesive forces and its effect on Ra. PC3 only associated characteristics of EOs such as the molecular weight of the prevailing compound and the EO melting point.

As described previously, natural waxes presented the largest structuring capacity and VRC of EOs. In order to verify if those results match those of the oil binding capacity (OBC), the mint and petitgrain EOs were chosen as model oils. In fact, all of them resulted in OBC larger than 97% which were very close to those of VRC indicating a high resistance of these matrixes to oil dripping (Table 2).

Table 2: Oil binding capacity of matrixes produced with selective essential oils and natural waxes

Essential oil	Natural wax	Oil binding capacity (%)
Mint	Beewax	100
	Candelilla wax	100
	Ozokerite wax	100
	Carnauba wax	99
Petitgrain	Beewax	100
	Candelilla wax	100
	Ozokerite wax	100
	Carnauba wax	97

CONCLUSION

EO structuring into a lipidic matrix depended mostly on the magnitude of the hydrogen forces of EOs and their interactions with the emulsifier. If such interactions are repulsive it is expected a high crystallization followed by gelation when fatty emulsifiers are involved. Conversely, polymeric emulsifiers having a high hydrogen bonding forces rapidly structured oils via swelling especially with EOs having large hydrogen bond forces such as geranium, organum, basil, clove and cinnamon.

Acknowledgement-This work was sponsored by Colciencias through the grant 755-2017 for the formation of Colombian PhDs. The authors also thank the committee for the development of research (CODI) of University of Antioquia and its Sustainability Strategy Program (2018-2019) for their financial support.

Conflicts of interest-Nil

REFERENCES

- Dagli, N., Dagli, R., Mahmoud, R.S., Baroudi, K., Essential oils, their therapeutic properties, and implication in dentistry: A review. *Journal of International Society of Preventive & Community Dentistry*. 2015, 5, 335-340.
- Raut, J.S., Karuppayil, S.M., A status review on the medicinal properties of essential oils. *Industrial Crops and Products*. 2014,62, 250-264.
- Karrapandzova, M., Stefkova, G., Cetkovikl, I., Trajkovska-dokik, E., Kaftandzieva, A., Kulevanova S., Chemical composition and antimicrobial activity of the essential oils of *Pinus peuce* (Pinaceae) growing wild in R. Macedonia. *Natural Product Communications*. 2014, 9, 1623-1628.
- Gao, J., Wu, S., Rogers, M., Harnessing Hansen solubility parameters to predict organogel formation. *Journal of Materials Chemistry A*. 2012, 22, 12651-8.
- Hansen, C.M., 50 Years with solubility parameters-past and future. *Progress in Organic Coatings*. 2004, 51, 77-84.
- Hansen, C.M., The universality of the solubility parameter. *Industrial & Engineering Chemistry Research*. 1969, 8, 2-11.
- Senichev, V., Tereshatov, V., General principles governing dissolution of materials in solvents., in *Handbook of Solvents*. ChemTech Publishing, Edition 3, Vol. I, 2019:133-275.
- Hansen, C.M., Hansen solubility parameters: a user's handbook: CRC press; 2002.
- Davidovich-Pinhas, M., Barbut, S., Marangoni, A., The gelation of oil using ethyl cellulose. *Carbohydrate Polymers*. 2015, 117, 869-78.